

## 6. SITE 279

### The Shipboard Scientific Party<sup>1</sup>

#### SITE DATA

**Location:** Northern Macquarie Ridge

**Position:** 51°20.14'S; 162°38.10'E

**Water Depth:**

PDR, from sea level: 3341 meters

From drill pipe measurement from derrick floor: 3381 meters (adopted)

**Dates Occupied:** 20-22 March 1973

**Depth of Maximum Penetration:**

Hole 279: 1 meter

Hole 279A: 202 meters

**Number of Holes:** 2

**Number of Cores:**

Hole 279: 1

Hole 279A: 13

**Total Length of Cored Section:**

Hole 279: 1.0 meter

Hole 279A: 110 meters

**Total Recovery:**

Length:

Hole 279: 0.6 meter

Hole 279A: 79.8 meters

Percentage:

Hole 279: 60

Hole 279A: 72.5

**Age of Oldest Sediment Cored:** Middle early Miocene

**Summary:** Thin (13 m) Pleistocene veneer of foraminifera ooze overlies erosional surface, beneath which is 185 meters of late middle Miocene to middle early Miocene foraminifera-bearing nannofossil ooze. Ash-rich at base of section. Excellent foraminiferal and nannofossil sequence. Abundance of discoasters at some Miocene intervals indicates surprising warmth for this latitude. Apparently continuous sequence with constant sedimentation of about 1.85 cm/1000 years. Cored 4 meters of vesicular basalt. Sediment overlying basement is 20 m.y. old (middle early Miocene). Unconformity near surface records increased

<sup>1</sup>James P. Kennett, Graduate School of Oceanography, University of Rhode Island, Kingston, Rhode Island; Robert E. Houtz, Lamont-Doherty Geological Observatory of Columbia University, Palisades, New York; Peter B. Andrews, New Zealand Geological Survey, Christchurch, New Zealand; Anthony R. Edwards, New Zealand Geological Survey, Lower Hutt, New Zealand; Victor A. Gostin, University of Adelaide, Adelaide, Australia; Marta Hajós, Hungarian Geological Survey, Budapest, Hungary; Monty Hampton, University of Rhode Island, Kingston, Rhode Island; D. Graham Jenkins, University of Canterbury, Christchurch, New Zealand; Stanley V. Margolis, University of Hawaii, Honolulu, Hawaii; A. Thomas Owen-shine, U.S. Geological Survey, Menlo Park, California; Katharina Perch-Nielsen, Institut for Historisk Geologi, Copenhagen, Denmark.

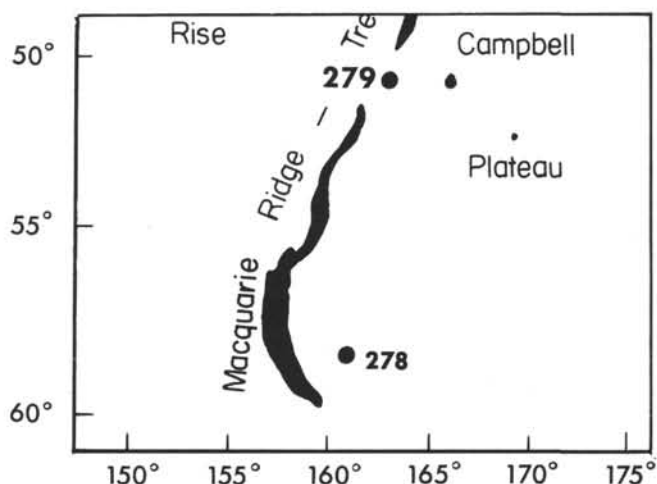


Figure 1. Location of Site 279, DSDP Leg 29.

late Cenozoic bottom erosion in deeper parts of the southern Tasman Sea region previously observed in many piston cores but extends knowledge of erosion to shallow water associated with ridge.

#### BACKGROUND AND OBJECTIVES

At Site 279 about 240 meters of pelagic ooze was continuously-semicontinuously cored in a thin sediment pocket on the northern part of the Macquarie Ridge (Figures 1 and 2). Nearby the sediment cover is very thin or missing on a rough basement surface (Figure 3). The site was located in 3335 meters of water.

The most important objectives at Site 279 were:

1) To obtain basement age of part of the Macquarie Ridge. Several investigators have suggested that the Macquarie Ridge is a relatively young feature, no older than Miocene. They have also suggested that much of the movement on the Alpine Fault in New Zealand is genetically related to the development of the Macquarie Ridge. Drilling into basement and determining the age of basement placed much-needed constraints on these theories and shed light on the complex history of the Macquarie Triple Junction.

Determining the age of the Macquarie Ridge also has important paleo-oceanographic implications. The ridge presently diverts the circumpolar current and the Antarctic Convergence much further to the south than usual. Bottom-water circulation is also influenced by its presence. Dating of the Macquarie Ridge should assist in the understanding of the major paleocirculation

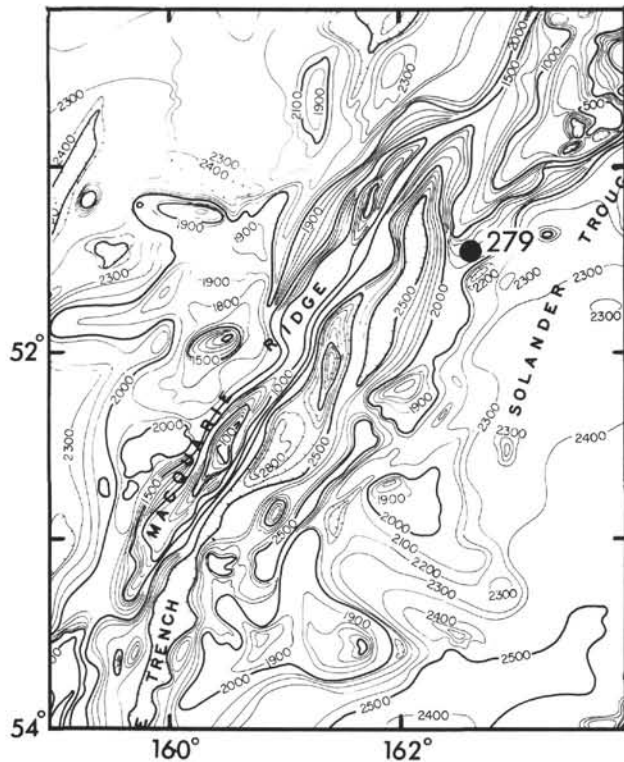


Figure 2. Bathymetry at Site 279.

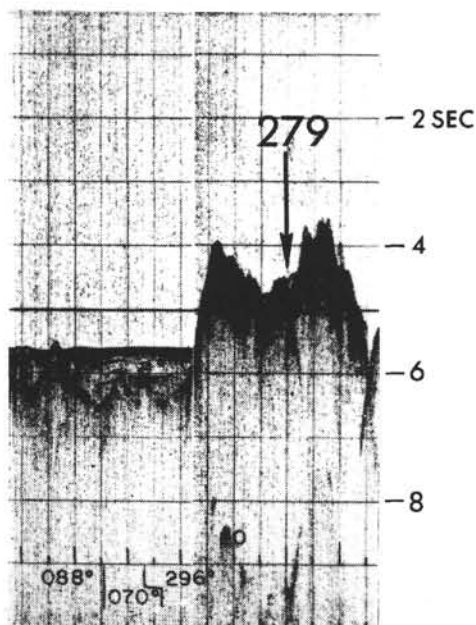


Figure 3. Profiler section at Site 279.

changes that have occurred during the Cenozoic in the southwest Pacific.

2) To obtain a late Cenozoic subantarctic biostratigraphic sequence.

**OPERATIONS**

Following an *Eltanin-53* track (Figure 4), Site 279 on the central Macquarie Ridge was approached from the southeast. The actual site was selected by sea-floor topography. A 13.5-kHz beacon was dropped while underway at 7.5 km/hr (4 knots) on the first pass over the site. The ship was unable to position over the beacon because of an erratic signal and loss of acoustics. A second 16-kHz beacon was dropped at 1050 hr.

Difficulties in positioning continued, and after an 8.5-hour delay the drill string was run in to a PDR depth of 3341 meters. A definite firm bottom was encountered at 3381 meters. Hole 279 was spudded with only 1 meter of penetration obtained with the maximum safe weight on the bit. Acoustics and positioning capability were lost; the drill string was pulled well clear of the sea floor, and the ship maneuvered to reposition over the beacon.

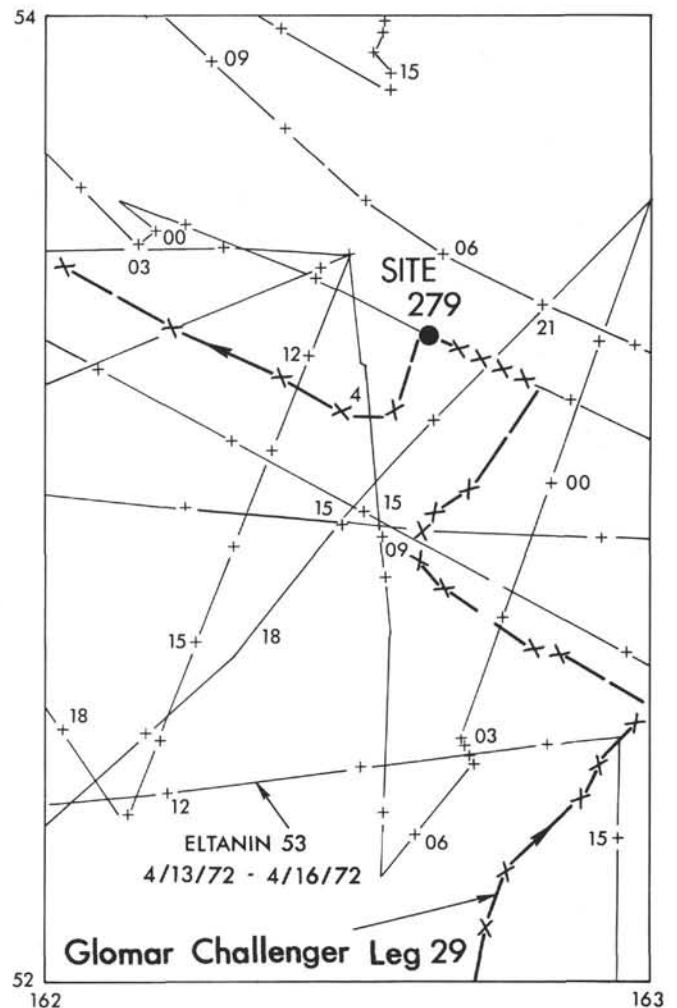


Figure 4. Track chart.

The drill string was run back in; a firm bottom was tagged at 3378 meters, 3 meters higher than Hole 279. Hole 279A was spudded, and washed down 13 meters before taking a core. Primarily to protect the bottom hole assembly, the hole was washed down to 3477 meters. From this depth the hole was continuously cored to a total depth of 3580 meters, 202 meters of penetration. Recoveries were somewhat erratic, but generally good with an overall recovery of 72.5%. Basement was encountered at 3575 meters (197 m penetration), recovering 3.4 meters of the 5 meters cored. Details of the coring are in Table 1.

TABLE 1  
Coring Summary, Site 279

Core	Cored Interval Below Bottom (m)	Cored (m)	Recovery (m)	Recovery (%)
<b>Hole 279</b>				
1	0.0-1.0	1.0	0.6	60
Total		1.0	0.6	60
<b>Hole 279A</b>				
1	13.0-20.0	7.0	6.0	86
2	99.0-108.5	9.5	2.5	26
3	108.5-118.0	9.5	9.5	100
4	118.0-127.5	9.5	2.8	30
5	127.5-137.0	9.5	5.2	55
6	137.0-146.5	9.5	9.5	100
7	146.5-156.0	9.5	9.5	100
8	156.0-165.5	9.5	4.5	47
9	165.5-175.0	9.5	9.5	100
10	175.0-184.5	9.5	7.9	83
11	184.5-194.0	9.5	9.5	100
12	194.0-199.0	5.0	1.2	24
13	199.0-202.0	3.0	2.2	73
Total		110.0	79.8	72

## LITHOLOGY

Holes 279 and 279A were drilled in a small depression near the crest of the Macquarie Ridge (Figure 2). Coring at Hole 279 resulted in the recovery of 105 cm of sediment. The sediment consisted of 35 cm of late Pleistocene or Recent foraminiferal nannofossil ooze unconformably overlying 70 cm of Miocene foraminifera-bearing nannofossil ooze. Hole 279A was drilled to a depth of 202 meters, penetrating 191 meters of sediment and 5 meters of basalt. The lithologic units encountered are listed in Table 2 and depicted in Figure 5. Table 3 summarizes the shipboard smear-slide determinations.

### Unit 1

The uppermost lithologic unit in both holes is very-light-gray soft to soupy nannofossil-foraminiferal ooze that is sandy in appearance because of the high proportion of foraminifera. Two smear slides from the unit show large variation in major components (Table 3). The lower contact of Unit 1 is deformed in both cores but the lithologic change appears to have occurred across a single bedding plane.

TABLE 2  
Lithologic Summary, Site 279

Unit	Lithology	Subbottom Depth (m)	Unit Thickness (m)
1	Nannofossil-foraminiferal ooze	0.0-13.3	13.3
2A	Interbedded gray and white foraminifera-bearing nannofossil ooze	13.3-109.4	96.1
2B	Homogeneous light gray foraminifera-bearing nannofossil ooze	109.4-137.0	27.6
2C	Foraminifera-bearing nannofossil ooze, trace detritus	137.0-169.7	32.7
2D	Mottled foraminifera-nannofossil ooze	169.7-173.4	3.7
2E	Foraminifera-bearing nannofossil ooze, trace detritus	173.4-187.7	14.3
2F	Detrital silty nannofossil ooze	187.7-189.7	2.0
2G	Discoaster-bearing silty nannofossil ooze	189.7-197.0	4.3
3	Vesicular fine-grained basalt	197.0-202.0	8.0

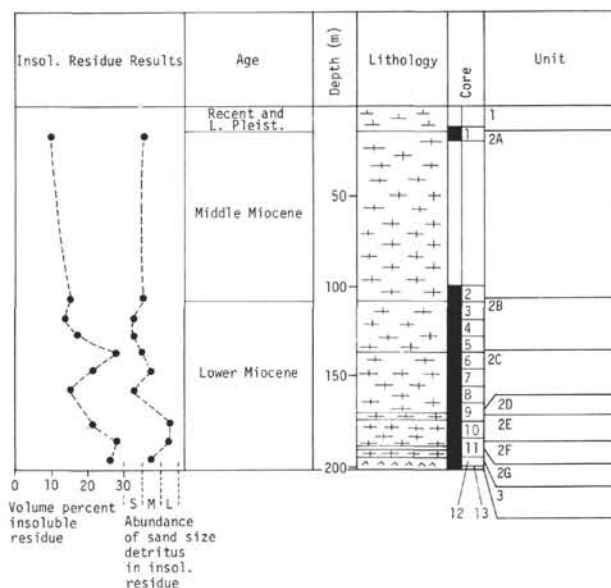


Figure 5. Stratigraphic sequence at Site 279.

At Hole 279, 0.3 meters of Unit 1, including the lower contact, was recovered; at Hole 279A, 0.3 meters at the lower contact was recovered, after washing through 13 meters of overburden. The apparent variation in thickness between two holes less than 100 meters apart suggests a disconformity at the base of Unit 1 that may have several meters of surface relief.

### Unit 2

Major changes in sediment composition do not occur in the cores recovered below the 13.3 meters (or less) of

**TABLE 3**  
Sediment Composition (percentage) Based on Smear-Slide Determination, Site 279

Sample (Interval in cm)	Diatoms	Radiolaria	Spicules	Nannofossils	Foraminifera	Discoasters	Glauconite	Micronodules	Authigenic Calcite	Zeolite	Chlorite	Detrital + Clay Minerals	Volcanic Glass	Basalt Rock Fragments	Pyroxene	Opaque Unknowns	Lithologic Unit
<b>Hole 279</b>																	
1-1, 65	tr	tr	2	78	20						tr						1
1, CC			1	84	9		1					5					2-A
<b>Hole 279A</b>																	
1-1, 140	4		4	30	45				15			2					1
1-2, 100	1	1	1	12	50				35			tr					
1-3, 130	tr	tr	1	80	8				10			1					
1, CC	tr	tr	2	88	10							tr					2-A
2-1, 105			1	84	15							tr					
2, CC			2	1	83	8			5			1					
3-3, 100	tr	tr	2	77	15		tr		5			1					
3-5, 43				84	15			1									
3-5, 84			1	84	15												
3-5, 130			1	83	10				5			1					
3-5, 144			2	82	10				5			1					2-B
3, CC	tr		2	78	20		tr				tr						
4-1, 110	tr	tr		90	5							5	tr				
4, CC		tr	1	93	3				2			1					
5-3, 100			3	90	6		tr	1			tr	tr					
5, CC			2	4	68	20			5			1					
6-1, 71		tr	2	88	10		tr					tr					
6, CC	2		1	86	5				5			1					
7-1, 106			1	92	7		tr										2-C
7, CC				87	8				5			tr					
8-4, 92			1	92	7							tr					
8-6, 149			1	88	5	2			4								
9-3, 136			1	93	5	tr	1					tr					
9-3, 144				76	15	2	1		4			1	1				2-D
9-5, 80			1	83	15	1	tr										
9-6, 125			3	80	9	2			3			3					
9, CC			1	87	8	1							3				2-E
10, CC			2	81	8	8						1					
11-3, 65				68					1					15	10	5	
11, CC				88	3	8	tr					tr	1				2-G

Note: tr = trace.

Recent foraminiferal ooze and above the top of the basalt at 197 meters subbottom. The samples from this interval consist of light-colored foraminifera-bearing nannofossil oozes in which calcareous nannofossils comprise about 85%. Thus Subunits 2A-2G are distinguished principally by changes in minor properties such as variation in color and structure and small changes in the proportions of foraminifera and terrigenous detritus. The unvarying composition of the major biogenic components and the apparently uniform sedimentation rate deduced indicate that the physical and biological factors controlling sedimentation remained essentially unchanged during deposition of the early and middle Miocene strata at Site 279.

**Subunit 2A**

Subunit 2A is known from 5.7 meters of core at the top of the unit and 2 meters of core near the base of the

unit. The contact with Subunit 2B was not recovered. The definition and description of Subunit 2A, 96.1 meters thick, is based on meager information.

Subunit 2A consists of interbedded light-greenish-gray foraminifera-rich nannofossil ooze and white foraminifera-bearing nannofossil ooze. These alternating lithologies differ principally in the preferential development of glauconite inside foraminifera tests in the greenish-gray foraminifera-rich nannofossil ooze. The composition of four smear slides from the subunit is shown on Table 3. An insoluble residue consists of basaltic lithic fragments, 45%; sponge spicules, 25%; glauconite, 20%; and plagioclase, 10%.

Paleontological methods have identified a major disconformity in the upper part of Subunit 2A. This disconformity (Sample 279A-1-3, 120 cm) is not marked by pronounced lithologic change other than a decrease in abundance of foraminifera, an increase in stiffness of the

sediment, and a slight change in color (white [N9] to white [10YR 7.5/1]).

#### Subunit 2B

Subunit 2B consists of 27.6 meters of light-gray micarb/foraminifera-bearing nannofossil ooze. The percentage composition of the subunit, based on an average of eight smear slides, is nannofossils, 85%; foraminifera, 10%; authigenic calcite, 2%; and minor amounts of sponge spicules, detrital grains, and clay. The average percentage composition of three insoluble residues is basaltic lithic fragments, 40%; siliceous tests and spicules, 30%; plagioclase, 16%; glauconite, 14%; and traces of pyroxene and biotite(?). The total insoluble residue, which includes clay minerals and much organic matter, comprises 15% of the sediment volume.

Bedding and other primary sedimentary features are well displayed in Core 279A-5, Section 4. Bedding is generally at a scale of 10-20 cm thick, and is best recognized as alternations of soft and stiff intervals. Within individual beds about 50% of the sediment lacks primary sedimentary structures, 40% exhibits faint mottling caused by burrowing organisms, and about 10% displays fine laminations 0.5-3 meters thick. Burrows are typically 2-5 mm wide, and less than 10 mm long.

Neither contact of Subunit 2B is exposed for detailed examination: a small void occurs above the first appearance of the lithology in Core 3-1, and the lower contact apparently occurs in Sample 279A-5, CC.

#### Subunit 2C

Subunit 2C consists of light-gray micarb- and foraminifera-bearing nannofossil ooze, with small but discernible amounts of glauconite, and sand- and silt-sized volcanic detritus. Under the hand lens the glauconite and volcanic detritus impart a "peppered" appearance to the sediment. The composition of seven smear slides is shown in Table 3. Insoluble residues from Cores 6 and 7 comprise 20% and 15% of the sediment volume, and consist primarily of organic matter and clay. Residues from which the clay and organic matter have been removed consist of spicules and siliceous tests, 47%; glauconite, 22%; basaltic rock fragments, 15%; feldspar, 15%; and minor amounts of glass shards, pyroxene, and anorthoclase(?).

Subunits 2B, 2C, 2E, and 2G display cyclic alternations of sediment consistency. Stiff to semi-indurated zones 5-15 cm thick alternate with soupy to soft intervals 10-50 cm thick. Density increases of 0.1-0.2 g/cc correlate with the more consolidated zones on some GRAPE records, but on many other records a close correspondence is not discernible. Paired smear slides from "hard" and "soft" intervals do not show gross compositional differences between the zones, but in many cores, zones of intense bioturbation correlate closely with the more consolidated layers. These variations in sediment consistency appear to be primary properties of the sediment and not drilling artifacts; their origin, however, is unknown.

#### Subunit 2D

Subunit 2D consists of 3.7 meters of light-gray glauconite- and foraminifera-bearing nannofossil ooze

with distinctive yellowish-gray mottles composed of glauconite-bearing foraminifera-rich nannofossil ooze. The mottled areas, which owe their yellowish color to oxidized glauconite, are irregular to ovoid in shape and 0.5-2 cm in diameter. The composition of Subunit 2D, from three smear slides, is shown in Table 3.

#### Subunit 2E

The yellowish gray mottling that distinguishes Subunit 2D diminishes with depth and vanishes at the top of Subunit 2E (Sample 279A-9-6, 40 cm). Subunit 2E consists of light-gray, soft to stiff foraminifera-bearing nannofossil ooze that is homogeneous and even-textured in appearance. The composition from three smear slides is shown on Table 3. The abundant sand-sized fraction of two insoluble residues consists of basaltic rock fragments, 43%; feldspar, 25%; spicules, 12%; brown volcanic glass, 10%; glauconite, 10%; and pyroxene, 5%. The total insoluble residue, including clay and organic matter, from two samples of Subunit 2E comprises 20% and 26% of the sediment volume.

The sediments of Subunit 2E are intensely bioturbated by round, ovoid, or irregular burrows 0.5-1 cm in size. Burrow fillings commonly are lighter gray than the surrounding sediment, and tend to show discrete margins. The trace fossil *Zoophycos* occurs sparingly.

#### Subunit 2F

Subunit 2F consists of 2 meters of intercalated dark-gray detrital sand and silt nannofossil ooze, and very-light-gray nannofossil ooze. The intercalations are of three types: (1) 10-15 cm thick beds; (2) dark-gray mottling probably bioturbate in origin (Figure 6); and (3) dark-gray unconsolidated intraclasts, some of which have been burrowed by the trace fossil *Zoophycos*.

Subunit 2F is rich in angular sand- and silt-size detritus that is predominantly of volcanic composition, but includes significant quantities of iceberg transported quartz. A smear slide from the subunit consists of nannofossils, 68%; basaltic rock fragments, 15%; pyroxene, 10%; opaque minerals, 5%; zeolite(?), 1%; and glauconite, 1%. At places the detrital constituents comprise more than half of the grain volume and impart a gray color to the sediment.

Subunit 2F probably originally consisted of alternating layers of detrital sandy silt and relatively pure nannofossil ooze. The activities of burrowing organisms and possibly of bottom currents have resulted in the present complexly mottled intercalated appearance of the sediment (Figure 6).

#### Subunit 2G

Subunit 2G consists of very-light-gray, stiff-to-soft, discoaster-bearing coccolith ooze. A smear slide from the subunit yields the following percentage composition: coccoliths, 88%; forams, 3%; discoasters, 8%; volcanic glass, 1%; and minor amounts of detrital constituents and glauconite. Acid-insoluble material comprises 26% of the sediment by volume. The sand-size insoluble fraction is composed of basaltic rock fragments, 40%; plagioclase, 23%; glauconite, 15%; pyroxene, 10%; siliceous spicules and tests, 10%; and shards, 2%.

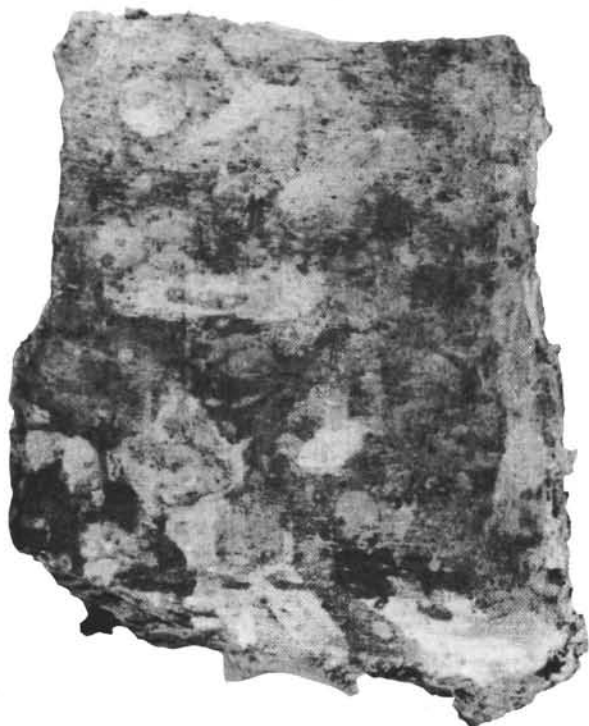


Figure 6. *Intensely mottled detrital sand and silt nanno ooze. Dark areas rich in detritus have been mixed with light-colored nanno ooze by the activity of burrowing organisms (X1).*

Sediments of the subunit exhibit both bioturbation and millimeter-scale horizontal lamination. The upper contact of the unit is a sharp bedding plane boundary; the lower contact with basalt was not recovered.

### Unit 3

Unit 3 consists of three sections of fine-grained dark-gray basalt. The basalt of Section 12-1 is vesicular to amygdaloidal, subaphanitic to very-fine-grained plagioclase-porphyritic basalt that grades to non-vesicular and non-porphyritic fine-grained basalt toward the base of the core. The basalt of Sections 13-1 and 13-2 is in lithic continuity with the vesicular basalt of Section 12-1, but differs from it in its slightly coarser grain size and lack of vesicles and phenocrysts. The non-vesicular basalt is subfriable and many of the short core segments have been abraded to barrel shapes during drilling.

In the upper 30 cm of Section 12-1, vesicles and amygdules comprise up to 40% of the rock volume. The vesicles are 0.5-4 mm in diameter, averaging 1.5 mm, with approximately 50% of the vesicles unfilled. The remaining 50% are partly to completely filled with white

calcite, chlorite, or a gray-blue zeolite(?). Pyrite subhedra occur sparingly in some.

In hand specimen the basalt of Section 12-1 has a color index of 70, and consists of 1% white plagioclase phenocrysts ranging to 4 mm in length in a subaphanitic to very-fine-grained groundmass that consists of equal parts of feldspar laths and pyroxene plus glass(?). In this section, the basalt of Section 13-2 has an intersertal texture, and consists of 0.2-0.4 mm labradorite laths, 35%; anhedral pyroxene, 30%; patches of partially altered crystallite-rich brown glass, 25%; and magnetite, 10%. Accessory minerals are calcite, chlorite, analcite(?), and an unidentified zeolite. Basalt from the vesicular part of Section 12-1 is similar, but the intercrystalline glass has fewer crystallites and is less altered.

The basalt recovered at Hole 279A is interpreted as the upper few meters of a lava flow.

### Insoluble Sand-Size Residues

At Hole 279A, hydrochloric-acid-insoluble residues were routinely prepared from core catcher samples to estimate detrital clay, silt, and sand content of sediments overwhelmingly biogenic in origin. Identifying detrital components is particularly difficult in nannofossil-rich sediments because the nannofossils will adhere to detrital grains. The results of this inquiry are presented in Figure 5. Two types of data are presented. Volume percent insoluble residue and the abundance of sand-size detritus.

The proportion of insoluble residue increases with depth at Hole 279A, with one peak in Subunit 2C between 137 and 150 meters and a second larger peak in Subunits 2D, E, and F between 170 and 190 meters.

The composition of the insoluble residues has not been studied in detail but the greatest proportion of the total insoluble residues appears to consist of clay and glauconite, spicules and siliceous tests, and brownish, isotropic organic matter. In the sand-size fraction, lithic fragments (derived from basalt mesostasis) and calcic feldspar predominate; pyroxene and brown volcanic glass occur in trace amounts throughout the core and are especially prominent in Subunits 2F and G.

Since the curves for total insoluble residue and sand-size components are sympathetic, and clays are major constituents of the total residues, the clay minerals are interpreted as being detrital in origin. The sand-size constituents are consistent with a basaltic source area which may have been the Macquarie Ridge. If this is correct, then the main episodes of volcanism associated with formation of the Macquarie Ridge occurred during the time of deposition of Subunits 2G through 2C.

### GEOCHEMICAL MEASUREMENTS

Table 4 and Figure 7 summarize the analyses of interstitial waters from the cores of Hole 279A. All pH measurements were lower than that of the surface seawater; alkalinities varied from a high of 3.03 meg/kg in the Core 1 to a low of 1.27 meg/kg in Core 11; and salinities were all higher than that of the surface seawater reference (34.4 ‰), with a high of 35.2 ‰ being found in Core 6.

TABLE 4  
Shipboard Geochemical Data, Hole 279A

Core	Section	Sample Interval		pH		Alkalinity (meq/kg)	Salinity (‰)	Lithologic Unit
		Top (m)	Avg (m)	Punch- in	Flow- thru			
Surface Seawater Reference				7.86	7.97	2.44	34.4	
1	3	13.0	17.03	7.37	7.45	3.03	34.9	2A
2	2	99.0	107.05	7.52	7.61	2.25	34.9	2A
3	4	108.5	113.53	7.62	7.65	2.25	34.9	2B
6	6	137.0	145.03	7.50	7.71	1.76	35.2	2C
11	5	184.5	192.47 <sup>a</sup>	7.68	7.81	1.27	34.9	2E
Average				7.54	7.63	1.99	34.9	

<sup>a</sup>Two analyses were run, the second on #50 Whatman filter paper. Values are: Flow-thru pH=7.58, Alk=1.37, and S=34.9‰

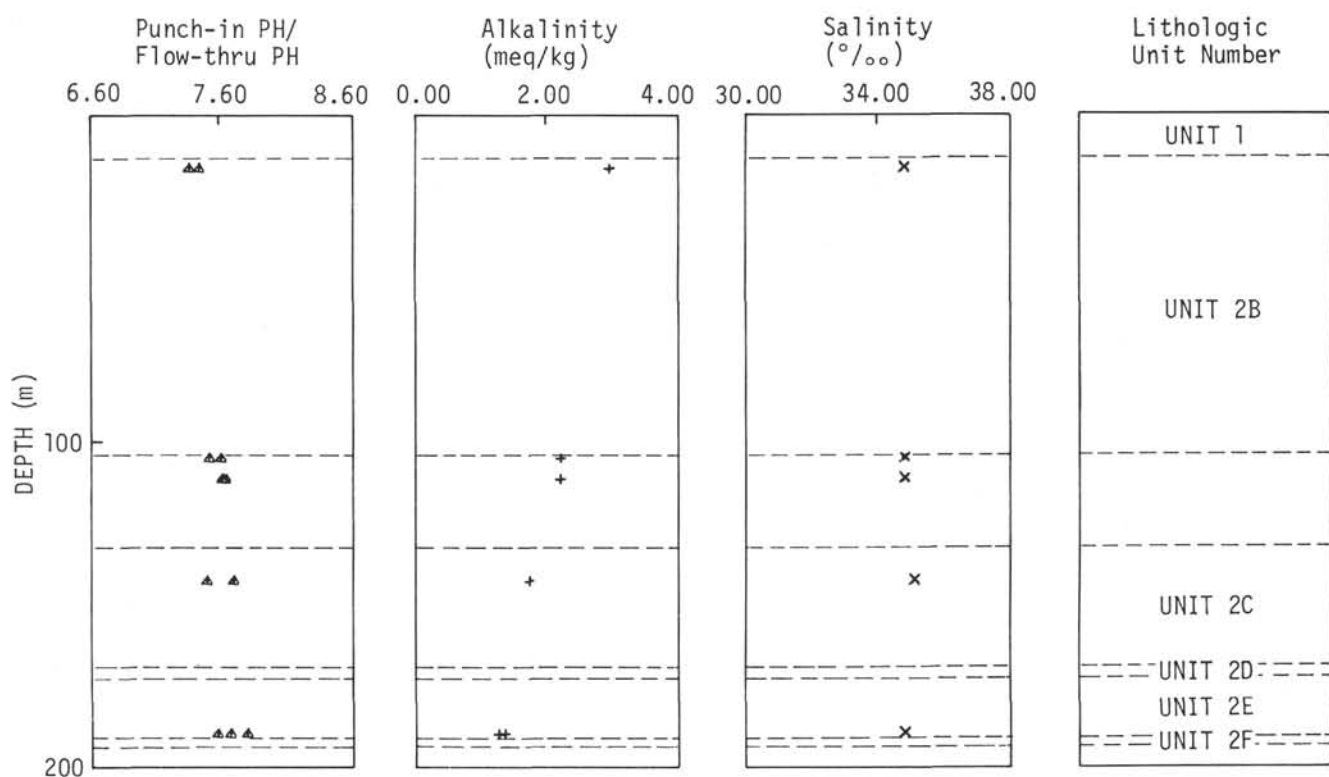


Figure 7. Shipboard geochemical data versus depth, Site 279.

### BIOSTRATIGRAPHY

The dominantly calcareous sequence at Holes 279 and 279A yielded abundant calcareous nannofossils and planktonic foraminifera. Siliceous fossils are sparse with more recorded diatoms than Radiolaria.

Above an unconformity seen in both Cores 279-1 and 279A-1, the Pleistocene to Recent(?) fossils are well preserved, and show no signs of solution.

Immediately beneath the unconformity, the hole penetrated the middle Miocene *Globorotalia (T.) mayeri* Zone which is well documented both in south-east Australia and New Zealand, and the nannofossil

*Reticulofenestra pseudumbilica* Zone. Below Core 279A-1 the hole was washed down 69 meters, with coring recommencing in the lower part of the middle Miocene planktonic foraminiferal *Praeorbulina glomerosa curva* Zone.

The main part of the cored sequence, Cores 279A-3 to 279A-11 is of early Miocene age according to both the planktonic foraminifera and calcareous nannofossils. Core 279A-11 penetrated the upper part of the *Globigerina (G.) woodi connecta* Zone, and the *Discoaster deflandrei* Zone. These are the lowermost zones in the New Zealand early Miocene.

The planktonic foraminiferal assemblages have been influenced by cool water, and show climatic fluctuations during the Miocene. The early Miocene yielded numerous nannoliths, but they are rare in the mid Miocene, a change which has been interpreted as due to a gradual climatic cooling through the Miocene. The paucity of siliceous microfossils is a notable feature of the site, with the exception of a richer and better-preserved lower Miocene diatom assemblage in Core 279A-9.

### Foraminifera

Sixty-five samples were examined. The Pliocene-Recent faunas are well preserved and the Miocene faunas are moderately well preserved, both faunas showing no signs of solution.

The Pleistocene-Recent fauna of the *G. (G.) truncatulinoides* Zone in Core 279-1 contains a few reworked specimens of the Pliocene-early Pleistocene *Globorotalia (T.) puncticulata*. A foraminiferal sand just above the unconformity in the upper part of Core 279A-1 has been dated as the Pliocene-Pleistocene *G. (T.) inflata* Zone.

The Miocene sediments in Hole 279A below the major unconformity have been divided into four middle and early Miocene planktonic foraminiferal zones which were previously established in southeast Australia and New Zealand (Jenkins, 1960, 1967), Table 5.

TABLE 5  
Planktonic Foraminiferal Zones, Site 279

Age	New Zealand Planktonic Foraminiferal Zones	Zonal Boundaries
Pleistocene	<i>G. (G.) truncatulinoides</i>	
Pleistocene-Pliocene	<i>G. (T.) inflata</i>	
	<i>G. (T.) mayeri mayeri</i>	
Middle Miocene	<i>P. glomerosa curva</i>	I.A. <i>P. glomerosa curva</i>
	<i>G. trilobus trilobus</i>	
Lower Miocene	<i>G. (G.) woodi connecta</i> (Upper)	I.A. <i>G. trilobus trilobus</i>

Note: I.A. = initial appearance

### *Globorotalia (G.) truncatulinoides* Zone

Core 279-1 yielded well-preserved specimens of 12 species of planktonic foraminifera typical of this latitude in surface sediment samples (Kustanowich, 1963). The Pleistocene age of the sample is based on the presence of *Globorotalia (G.) truncatulinoides* which has a well-developed keel and is left coiled. The boundary between the *G. (G.) truncatulinoides* Zone, and the *G. (T.) inflata* Zone has been placed between Samples 279-1-1, 87 cm, and 279A-1-1, 137 cm.

### *Globorotalia (T.) inflata* Zone

The fauna in the upper part of Core 279A-1 is less diverse and lacks *G. (G.) truncatulinoides* and is con-

sidered to be Pliocene-Pleistocene(?) in age. The boundary between the *G. (T.) inflata* and the *G. (T.) mayeri mayeri* zones has been placed between Samples 279A-1-2, 135 cm, and 279A-1, CC.

### *Globorotalia (T.) mayeri mayeri* Zone

The zone fossil is well developed and abundant. The species diversity is fairly high in the zone, comparable to the diversity recorded in New Zealand. The preservation is moderate to good throughout the zone. The boundary between the *G. (T.) mayeri mayeri* and the *P. glomerosa curva* zones has been placed between Samples 279A-1, CC, and 279A-2-1, 100 cm.

### *Praeorbulina glomerosa curva* Zone

The zone fossil is fairly rare and smaller than those in the zone in southeast Australia and New Zealand. The fauna is poor to moderately well preserved and the diversity not as high as the succeeding zone. Some of the warmer-water species, such as *Globigerinatella insueta*, found in New Zealand, are absent, being found only as far south as central North Island, New Zealand. The boundary between the *P. glomerosa curva* and the *G. trilobus trilobus* zones has been placed between Samples 279A-2, CC, and 279A-3-1, 130 cm.

### *Globigerinoides trilobus trilobus* Zone

The zone fossil is rare and sporadic in this zone, also rare in the succeeding zone, and is not present in the *G. (T.) mayeri mayeri* Zone. All the species found have previously been recorded from the *G. trilobus trilobus* Zone in southeast Australia and New Zealand (Jenkins, 1960, 1967). The diversity is moderate, the preservation moderate to good with some poor samples. The boundary between the *G. trilobus trilobus* and the *G. (G.) woodi connecta* zones has been placed between Samples 279A-10-3, 100 cm, and 279A-10-4, 135 cm.

### *Globigerina (G.) woodi connecta* Zone

Cores 279A-10 and 11 penetrated the upper part of the *G. (G.) woodi connecta* Zone, and below the initial appearance of *Globorotalia (T.) praescitula*. Some of the warmer-water species such as *Globigerinoides altiaperturus*, *Globorotalia (T.) obesa*, and *Globigerina ciperoensis* are not present. The diversity is moderate and fairly uniform, although an interval of low diversity coincides with an influx of detrital material, including quartz, in Sample 279A-11-3, 35 cm. The faunas are poor to moderately well preserved throughout with the best preservation coinciding with the high diversity in Sample 279A-11-4, 75 cm.

### Calcareous Nannofossils

This site provides abundant, fairly well preserved, and moderately diverse nannofloras throughout. The assemblages obtained indicate a sequence consisting of thin but complex latest Pleistocene, a very thin undifferentiated mid Pleistocene to late Pliocene, and a thick and almost continuous mid and early Miocene (Table 6). The substantially different surficial successions obtained from Holes 279 and 279A (Figure 8) suggests that the Miocene to late Pliocene or Pleistocene unconformity results from erosion controlled or modified by the

TABLE 6  
Calcareous Nannofossil Biostratigraphy, Site 279

Age	Zone	Hole 279	Hole 279A
Pleistocene	<i>C. pelagicus</i>	1-1, 50 to 99 cm	Above 1-3, 75 cm
	<i>Pseudoemiliana lacunosa</i>	Minor unconformity	Minor unconformity?
Pliocene		1-1, 99 to 03 cm	1-3, 75-120 cm(?) (see text)
Late Miocene	<i>Reticulofenestra pseudoumbilica</i>	Major unconformity	Major unconformity
		1-1, 103 cm to 1, CC	
Mid Miocene	<i>Cyclicargolithus neogammation</i>	Not drilled	1-3, 120 cm to 1-4, 30 cm
			1-4, 135 cm to 3-6, 106 cm
Early Miocene (part)	<i>Discoaster deflandrei</i> (part)		Minor unconformity(?)
			3-6, 106 cm to 11, CC

local bathymetry. The site appears to have been above the lysocline throughout the Neogene. The early Miocene nannofloras contain numerous nannoliths, which are very rare in the mid Miocene assemblages.

This situation is ascribed to a gradual upward climatic cooling from mid-subtropical to transitional-subantarctic conditions. The Pleistocene assemblages are consistent with the mid-subantarctic waters at present occurring above this site (Houtman, 1967).

The Pleistocene of this site is represented by two distinctly different successions, both of which abruptly overlie more compact mid-Miocene sediments (Figure 8). Hole 279 contains a highly condensed (49 cm) latest Pleistocene (*Coccolithus pelagicus* Zone with probable *Emiliana huxleyi*) sequence, which is basally underlain, probably unconformably (coincident with an abrupt sediment color change), by 3 cm of strongly winnowed undifferentiated mid Pleistocene to late Pliocene (*Pseudoemiliana lacunosa* Zone). Hole 279A contains about 17 meters of latest Pleistocene (*C. pelagicus* Zone with probable *E. huxleyi*) sediment underlain, (apparently conformably), by a thin interval of undifferentiated mid Pleistocene to late Pliocene (*P. lacunosa* Zone). Most of the samples yielded abundant, more or less diverse, and moderately well-preserved mid-subantarctic nannofloras. The effects of winnowing are conspicuous, especially in Samples 279-1-1, 100 cm and 279A-1-1, 25 cm; reworking occurs in a number of samples, notably 279-1-1, 60 cm. This situation is compatible with a late Neogene (Pliocene?) erosional channel which has recently aggraded to overflowing. If this supposition is correct, the apparent presence of the *P. lacunosa* Zone in Hole 279A could be a result of reworking of upslope sediments during the latest Pleistocene.

No definite Pliocene or late Miocene nannofloras have been recorded from this site. However, the possibility that the *P. lacunosa* Zone of Hole 279 represents a late Pliocene "lag deposit" cannot be excluded using only nannofossil evidence.

The mid Miocene is represented at this site by 98-112 meters of nannofossil ooze. Two zones can be recognized: a thin (about 14 meters thick) *Reticulofenestra*

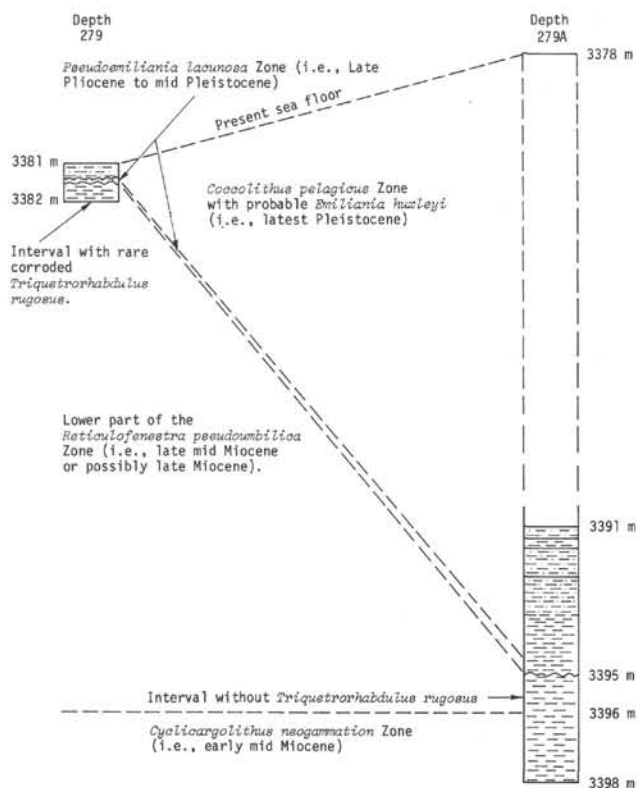


Figure 8. Calcareous nannofossil biostratigraphy of the surficial sediments at Site 279.

*pseudoumbilica* Zone, and an underlying much thicker (about 98 meters) *Cyclicargolithus neogammation* Zone. Elsewhere in the southwest Pacific, these zones are known to be undifferentiated early Pliocene to late mid Miocene, and early mid Miocene, respectively. Sequential position plus the sporadic occurrence of the Miocene nannolith *Triquetrorhabdulus rugosus* indicates a late mid Miocene or possibly a late Miocene age for the *R. pseudoumbilica* Zone. Two small specimens of the latest early Miocene to early mid Miocene nannolith *Sphenolithus heteromorphus* occur in the *C. neogammation* Zone in Sample 279A-3-3, 56 cm. The nannofloras of both of these zones are very abundant, fairly diverse, and more or less moderately well preserved. Only trace amounts of nannoliths (discoasters, sphenoliths, etc.) are present at the top of this interval, but discoasters are more numerous (but still rare) at the base of the mid Miocene. The frequency trend of *Helicopontosphaera* is almost identical to that of the discoasters. This situation suggests a gradual cooling from a cool subtropical climate in the early mid Miocene, to a transitional subantarctic climate in the late mid Miocene. The mid Miocene/early Miocene boundary by nannofossils coincides, within sampling limits, with a slight lithologic change (noticeable because of a color change) at Sample 279A-3-6, 106 cm. This coincidence could be due to a minor unconformity.

The early Miocene is represented by 81 meters of continuously cored nannofossil ooze containing nannofloras which conform to the *Discoaster deflandrei* Zone. Unfortunately no recovery was obtained from the 4 meters of sediment immediately overlying the vesicular basalt, but the overlying sediments yielded no evidence for the presence of pre-early Miocene strata in this sequence. The assemblages are very abundant and more or less diverse, but tend to be poorly preserved, especially in the basal 2 meters, where overgrowth is conspicuous. Nannoliths, a warm water group, are common throughout all but the uppermost part of this interval, but essentially consist of just four species: *Discoaster deflandrei*, *D. saundersi*, *D. adamanteus*, and *Sphenolithus moriformis* s.l. In the Tasman Sea area, assemblages containing substantial numbers of nannoliths almost invariably prove to be of early Miocene age. In the late Neogene such assemblages do not occur south of about 30°S, the present summer position of the tropical convergence. Thus, it seems probable that the summer surface water mass overlying Site 279 during the early Miocene was substantially warmer than at present; probably almost 20°C (i.e., a mid-subtropical climate). In both southeast Australia and New Zealand, the early Miocene was a period of near-tropical warmth with reef building corals in northern New Zealand, and common larger foraminifera as far south as a locality just 5° north of Site 279 (Hornibrook, 1971). In view of the sparse occurrence of nannoliths in the early Miocene of Site 278, 6° south of Site 279, it seems likely that a large thermal gradient similar to that occurring today existed between these two sites.

#### Diatoms

Twenty-six samples from Holes 279 and 279A were analyzed for diatoms. The samples were examined as

smear slides; as cleared material without sieving. Core catchers from Hole 279, and 279A-7, -8, -10, and -12 are barren. Most of the other samples from Hole 279A contain very few, poorly preserved diatoms, making identification difficult. Exceptions are Samples 279A-9-6, 118-120 cm, and 279A-9, CC.

The poor assemblages of diatoms occurring in Sample 279A-1-1, 118-120 cm have been examined and documented as a Pleistocene-Recent flora. Samples 279-1-2, 118-120 cm, 279-1-3, 118-120 cm, and 279-1-4, 118-120 cm were taken from Pliocene-Pleistocene sediments. *Fragilariopsis kerguelensis*, *Synedra jouseana*, *Coscinodiscus lentiginosus*, and *C. tabularis* are common in these samples. *Dimidium falcatum* n. sp. n. genus is common only in Sample 279-1-2, 118-120 cm. All these are characteristic cool-water planktonic species.

The poor assemblages of planktonic diatoms occurring in Sample 279-1, CC and Core 279A-2 are of middle Miocene age based on the occurrence of *Actinocyclus ingens*, *A. tsugaruensis*, *Coscinodiscus excetricus*, *C. oculus-iridis*, *Hemidiscus karstenii*, *Thalassiothrix longissima*, and *Triceratium fавus*.

Poorly preserved and sparse early Miocene diatom floras occur in Cores 3 to 9 but are difficult to identify. Exceptions are the floras in Samples 279A-9-6, 118-120 cm, and 9, CC. These samples contain common *Melosira (Paralia) sulcata*, *Stephanopyxis turris*, *Thalassionema nitsschioides*, and *Triceratium cellulosum* var. *japonica*. All these are warmer-water species. These and the occurrence of *Distephanus crux*, and other silicoflagellates species such as *Corbisema triacantha* and *Mesocena* sp., indicate that the early Miocene was much warmer than the Plio-Pleistocene.

#### Radiolaria

Radiolaria are rare and poorly preserved in Samples 1, CC to 7, CC. A few fragments occur in Sample 8, CC. No Radiolaria were found below this level.

#### SEISMIC DATA

Profiler data at the site show acoustically transparent sediments deposited in mound-like structures, indicative of very soft sediments. Locally, however, the sea floor is quite reflective, especially in concave focussing situations (Figure 3). Basement, at 197 meters subbottom, corresponds to a reflection time of 0.23 sec. The mean sediment sound velocity is 1.72 km/sec.

#### SEDIMENTATION RATES

Sedimentation rates (Figure 9) within the Miocene sequence at Site 279 are based on only three biostratigraphic horizons that could be correlated with the radiometric time scale; hence, conclusions are tentative. The relatively uniform foraminifera-rich nannofossil oozes that make up the entire Miocene sequence have an average measured sedimentation rate of about 2 cm/1000 yr, normal for this type of deposit. Density measurements carried out through the sequence indicate that before compaction initial sedimentation rates are 10% greater than measured rates. A minor unconformity could be present in Sample 279A-3-6, 106 cm, suggested by the coincidence of a slight lithologic change, and the mid Miocene-early Miocene boundary determined by

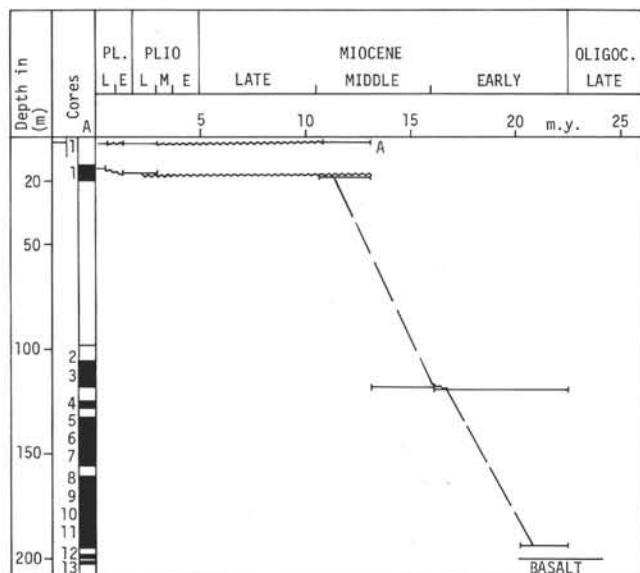


Figure 9. Sedimentation rate curve at Site 279; the same sequences were found in Holes 279 and 279A but at different depths.

nannofossils. The major unconformity separating middle Miocene from late Pliocene to early Pleistocene, and a minor unconformity within the Pleistocene are shown in Figure 9.

Increased bottom water in the region during the late Cenozoic has removed most of that part of the sequence, although some late Pliocene to early Pleistocene, and a veneer of Pleistocene foraminiferal ooze have been subsequently deposited.

### SUMMARY AND CONCLUSIONS

Site 279 was drilled in a small depression on the eastern flank of the Macquarie Ridge in a water depth of 3378 meters. At Hole 279 only one surficial core (105 cm) was obtained. This consisted of 35 cm of Pleistocene-Recent foraminiferal ooze unconformably overlying 70 cm of middle Miocene foraminifera-bearing nannofossil ooze. Hole 279A was drilled to a depth of 202 meters, penetrating 197 meters of sediment and 5 meters of basalt. Three units were distinguished: a Pleistocene veneer (13.3 m) of nannofossil-foraminifera ooze with reworked Miocene nannofossils (Unit 1), is underlain by a thick (183.7 m) sequence of nannofossil ooze (Unit 2). A major unconformity within Unit 2 separates 1.2 meters of Pleistocene sediment from 182.5 meters of middle to middle early Miocene sediment. This in turn is underlain by vesicular, fine-grained basalt (Unit 3). The difference in thickness of the Pleistocene sediments between Holes 279 and 279A suggests that the erosional surface developed on the Miocene is irregular and covered by varying thicknesses of Pleistocene sediments.

Major changes in sediment character do not occur within Unit 2, which consists of light-colored foraminifera-bearing nannofossil oozes in which calcareous

nannofossils consistently average about 85% of the sediment. Unit 2 is subdivided into seven subunits based on differences in minor properties such as color and structure, in the proportions of foraminifera and terrigenous and volcanic detritus.

Sedimentation rates for the Miocene sequence are about 2 cm/1000 yr which is normal for this type of sediment. An uncored interval of 69 meters between 20 and 99 meters is middle Miocene, and the observed biostratigraphic progress suggests a constant sedimentation rate over this uncored interval.

The section contains an important sequence of well-preserved to moderately well-preserved calcareous nannofossils and planktonic foraminifera. Siliceous fossils are scarce.

Unit 3 is 5 meters of fine-grained dark-gray basalt that is vesicular and porphyritic only in the upper part and interpreted as the upper few meters of a lava flow, although the basalt-sediment contact was not obtained.

### Conclusions

Site 279 represents a sequence of nannofossil oozes that shows relatively uniform, slow rates of sediment deposition throughout the early and middle Miocene with no apparent breaks in sedimentation. Preservation of the calcareous biogenic components indicates deposition above the lysocline. The unvarying composition of the major biogenic components and rather uniform sedimentation rates indicate that the physical and biological properties controlling sedimentation remained essentially unchanged during the early and middle Miocene. Increased activity of the bottom water in the region has removed the upper Cenozoic although a veneer of Pleistocene-Recent foraminiferal ooze has subsequently been deposited. Moderate compaction of the Miocene nannofossil ooze indicates a previous overburden was present. This late Cenozoic erosion is widespread in the southern Tasman Sea region from studies of piston cores, but this is the first recording of the unconformity in shallower waters associated with the Macquarie Ridge.

Large fluctuations of discoasters during the Miocene reflect climatic variations and their abundance in some intervals implies surprising warmth for this latitude. Preliminary investigations of quartz-grain surface features with a light microscope imply that iceberg-transported grains occur at various intervals in the early Miocene. The association of volcanic detritus with the quartz suggests that the volcanic detritus was also transported by icebergs. However, studies of the glacial quartz grains with the scanning electron microscope may reveal that they have been transported by bottom currents from another area along with the volcanic detritus (Chapter 30, this volume).

The sampling of early Miocene sediments directly overlying a fine-grained vesicular basalt at Site 279 indicates that the Macquarie Ridge was probably (but not necessarily) beginning to form at that time. This basalt is therefore about 25 m.y. younger than the sea floor just west of the ridge, at the same latitude (Weissel and Hayes, 1972).

The older sea floor to the west of the ridge is barren of sediment 50-100 km from the ridge. Farther west the sediments are entirely pelagic, in marked contrast to the ponded turbidites east of the ridge. The ridge has been an effective barrier between the two sediment regimes during the past 20 m.y. Dating the initial formation of the ridge also dates the probable onset of strike-slip motion along the Alpine fault in New Zealand.

The middle early Miocene age of the Macquarie Ridge is younger than major paleocirculation changes that occurred in the southeast Pacific during the Oligocene. Before the late Oligocene, erosive bottom waters were active in the northern Tasman Sea-Coral Sea areas, after which they were diverted to areas south and east of New Zealand and have been important in this region throughout the Neogene. The development of the Macquarie Ridge does not coincide with and thus probably did not cause these changes.

Presently the Macquarie Ridge diverts the circumpolar current far to the south. The development of the ridge in the early Miocene does coincide with the first appearance of diatom-rich sediments at Site 278 in the Emerald Basin near the southern part of the ridge. These two events are probably unrelated because if the ridge diverted warmer waters to the south soon after develop-

ment, as it does in the present day, calcareous biogenic sediments should be dominant at Site 278 in the early Miocene, if other oceanographic changes such as the migration or development of the Antarctic Convergence had not occurred.

#### REFERENCES

- Hornibrook, N. de B., 1971. New Zealand Tertiary climate: New Zealand Geol. Surv. Report 47, p. 1-19.
- Houtman, T. J., 1967. Water masses and fronts in the Southern Ocean south of New Zealand: New Zealand Dept. Sci. Indus. Res. Bull. 174, p. 1-40.
- Jenkins, D. G., 1960. Planktonic foraminifera from the Lakes Entrance oil shaft, Victoria, Australia: *Micro-paleontology*, v. 6, pt. 4, p. 345-371.
- , 1967. Planktonic foraminiferal zones and new taxa from the lower Miocene to the Pleistocene of New Zealand: *New Zealand J. Geol. Geophys.*, v. 10 (4), p. 1064-1078.
- Kustanowich, S., 1963. Distribution of planktonic foraminifera in surface sediments of the southwest Pacific Ocean: *New Zealand J. Geol. Geophys.*, v. 6 (4), p. 534-565.
- Weissel, J. and Hayes, D., 1972. Magnetic anomalies in the southeast Indian Ocean: *In* Hayes, D. E. (Ed.), *Antarctic Oceanology II: The Australian-New Zealand Sector*, Antarctic Res. Ser., v. 19, Am. Geophys. Union, p. 371-395.

**APPENDIX A**  
**Summary of X-Ray<sup>a</sup>, Grain Size, and Carbon-Carbonate Results, Site 279**

Section	Sample Depth Below Sea Floor (m)	Lithology	Age	X-Ray <sup>b,c</sup>									Grain Size				Carbon Carbonate			Comments
				Bulk Sample Major Constituent			2-20 $\mu$ Fraction Major Constituent			<2 $\mu$ Fraction Major Constituent			Sand (%)	Silt (%)	Clay (%)	Classification	Total (%)	Organic (%)	CaCO <sub>3</sub> (%)	
				1	2	3	1	2	3	1	2	3								
279A-1-1 279A-1-3	13.8-14.4 17.3	<b>Unit 2A</b> Foraminifera-bearing nannofossil ooze		Calc.	Mica	Plag.	Plag.	Quar.	Mica	Mica	Plag.	Mont.	10.5	47.1	42.4	Clayey silt	11.3	0.0	91	Amph in bulk fraction.
279A-3-6	117.1-117.2	<b>Unit 2B</b>		Calc.	*		Plag.	Quar.	Mica	Mont.	Mica	Quar.	4.7	54.1	41.2	Clayey silt	10.3	0.0	86	*Equal amounts of quartz, plag., Mica, Augite in 2-20 $\mu$ .
279A-4-2	120.3-120.4	Foraminifera bearing nannofossil ooze		Calc.	*	Quar.	Plag.	Quar.	Mica	Mont.	Quar.	Plag.	10.9	45.4	43.6	Clayey silt	9.9	0.0	82	*Equal amounts of Plag. and Mica, Augi. in 2-20 $\mu$ .
279A-5-4	132.7												0.3	38.3	61.4	Silty clay	9.5	0.0	79	
279A-6-5	144.3-144.5	<b>Unit 2C</b>		Calc.	Plag.	Augi.	Plag.	Quar.	Augi.	Mont.	Mica	Quar.	2.6	48.0	49.4	Silty clay	9.7	0.1	79	Augi in bulk, 2-20 $\mu$ , and <2 $\mu$
279A-7-5	153.1-153.2	Foraminifera-bearing nannofossil ooze		Calc.	Augi.	Plag.	Plag.	Quar.	K-Fe	Mont.	Quar.	Plag.	0.4	41.0	58.6	Silty clay	10.2	0.0	84	
279A-8-5	162.8-163.0			Calc.	Augi.	Plag.	Plag.	Quar.	Mont.	Mont.	Quar.	Plag.	7.0	57.0	35.9	Clayey silt	9.6	0.1	80	
279A-9-5	172.7-172.8	<b>Unit 2D</b> Foraminifera-nannofossil ooze		Calc.	Plag.	Quar.	Plag.	Quar.	Mont.	Mont.	Quar.	Mica	11.9	45.1	43.0	Clayey silt	10.2	0.0	85	Augi. in 2-20 $\mu$ ; Hali. in <2 $\mu$ .
279A-10-5	181.4-181.9	<b>Unit 2E</b> Foraminifera-bearing nanno ooze		Calc.	Plag.	Mont.	Plag.	Quar.	Mont.	Mont.	Hali.	Quar.	7.6	43.6	48.8	Silty clay	9.9	0.0	82	Augi. in 2-20 $\mu$ ; Hali. in <2 $\mu$ .
279A-11-6	192.5-193.0	<b>Unit 2G</b> Discoaster-bearing silty nannofossil ooze		Calc.	Mont.	Plag.	Plag.	Mont.	Quar.	Mont.	Plag.	Quar.	4.0	51.6	44.4	Clayey silt	10.2	0.0	84	Augi. in 2-20 $\mu$

Note: \* = see comment column.

<sup>a</sup>Complete results of X-ray, Site 279 will be found in Appendix I.

<sup>b</sup>Legend in Appendix A, Chapter 2.

<sup>c</sup>Peaks at 5.76Å, 3.63Å and 8.12Å found in bulk fraction of sections 279A-1-1, and 279A-8-5 (0-5%).





Site 279 Hole A Core 6 Cored Interval: 137.0-146.5 m

AGE	ZONE	FOSSIL CHARACTER		SECTION	METERS	LITHOLOGY	DEFORMATION	LITHO. SAMPLE	LITHOLOGIC DESCRIPTION
		FOSSIL ABUND.	PRES.						
EARLY MIOCENE	G. trilobus trilobus D. deflandrei	F N	C A	P M	1	VOID		-71	<p>Subunit 2C. A new lithologic unit begins in the core catcher of Core 5. Contact with the overlying strata not observed. Light gray (N7) FORAM-BEARING to FORAM-RICH NANNO OOZE (trace glauconite and detritals). Cycles of induration are prominent features and consist of a stiff-to semi-indurated base and a soft to soupy top. Repetition length of the cycles is 30-50 cm. This unit is distinguished from the overlying unit principally by its higher content in detrital sand and silt and its higher glauconite content. Under hand lens these constituents impart a "peppered" look and comprise 1 to 2% of the sediment.</p> <p>SS 1-71 SS CC SS CC                      N -88% N -86% (Insol.)                      F -10% (dis- S,St -50%                      S -2% coasters) G -30%                      Fd -TR M -5% BMs -10% (Plag.)                      Mi -TR F -5% Fd -10%                      G -TR Di -2% VG -TR                      R -TR S -1% HM -TR                      DE -1%                      (feldspar,                      mica,                      heavies,                      glass)</p> <p>X-ray 5-146 (Bulk)                      Calc - M                      Quar - TR                      Plag - P                      Mica - TR                      Augi - TR</p> <p>Grain Size 5-143 (2.6, 48.0, 49.4)                      Carbon Carbonate 5-130 (9.7, 0.1, 79)</p>
					2	VOID			
					3	VOID			
					4	VOID			
					5	VOID			
					6	VOID			
					Core Catcher			-CC	

Site 279 Hole A Core 7 Cored Interval: 146.5-156.0 m

AGE	ZONE	FOSSIL CHARACTER		SECTION	METERS	LITHOLOGY	DEFORMATION	LITHO. SAMPLE	LITHOLOGIC DESCRIPTION
		FOSSIL ABUND.	PRES.						
EARLY MIOCENE	G. trilobus trilobus D. deflandrei	F N	M A	P M	1	VOID		-106	<p>Lithologically identical to Core 6, Sec. 1 FORAM-BEARING to FORAM-RICH NANNO OOZE.</p> <p>SS 1-106 SS 1-106 SS CC SS CC                      N -92% (Insol.) N -87% (Insol.)                      F -7% G, Fd -7% S, St -45%                      S -1% (Plag.) M -5% Fd -20% (Plag.)                      G -TR OP - HM -TR BMs -20%                      (magnetite) R -TR G -14%                      HM - Si -TR VG -1%                      (pyroxene) OP -TR                      MI-TR -                      (chlorite,                      biotite)</p> <p>X-ray 5-65 (Bulk)                      Calc - M                      Quar - TR                      X-Fe - TR                      Plag - TR                      Augi - TR</p> <p>Grain Size 5-60 (0.4, 41.0, 58.6)                      Carbon Carbonate 5-70 (10.2, 0.0, 84)</p>
					2	VOID			
					3	VOID			
					4	VOID			
					5	VOID			
					6	VOID			
					Core Catcher			-CC	

Explanatory notes in Chapter 1





AGE	ZONE	FOSSIL CHARACTER		SECTION	METERS	LITHOLOGY	DEFORMATION	LITHO. SAMPLE	LITHOLOGIC DESCRIPTION
		FOSSIL ABUND.	PRES.						
				1	0.5 1.0	VOID			<p>Dark gray (N3) VESICULAR BASALT.</p> <p>The basalt recovered in Core 12-1 is vesicular to amygdaloidal very fine grained plagioclase porphyritic basalt that grades into non-vesicular non-porphyritic basalt with increasing depth in the core.</p> <p>In the upper 30 cm vesicles comprise up to 40% of the rock; near the base of the core they amount to less than 10%. The vesicles range from 0.5 to 4 mm in diameter, averaging 1.5 mm. An estimated 90% of the vesicles are unfilled, the remaining 10% are partly or completely filled with white calcite, chlorite or a blue zeolite(?). Pyrite subhedra occur sparingly in the amygdules.</p> <p>The basalt of Sec. 1 has a color index of 70 and consists of &lt;1% white plagioclase phenocrysts ranging to 4 mm in length in a subaphanitic groundmass that appears to consist of feldspar laths (60%), pyroxene and glass(?) (40%).</p>

AGE	ZONE	FOSSIL CHARACTER		SECTION	METERS	LITHOLOGY	DEFORMATION	LITHO. SAMPLE	LITHOLOGIC DESCRIPTION
		FOSSIL ABUND.	PRES.						
				1	0.5 1.0	VOID			<p>Fine grained basalt in lithic continuity with the basalt of Core 12, Sec. 1, but differing from it by the lack of phenocrysts and vesicles and by a slightly coarser grain size. Core segments are "soft" - almost friable - and have a pronounced barrel-shape as a result of abrasion.</p>
				2					

Explanatory notes in Chapter 1

